

# Frontier molecular orbitals of single molecules adsorbed on thin insulating films supported by a metal substrate: A simplified density functional theory approach

Iván Scivetti<sup>1</sup> and Mats Persson<sup>12</sup>

<sup>1</sup> Surface Science Research Centre and Department of Chemistry University of Liverpool Liverpool L69 3BX UK

<sup>2</sup> Department of Applied Physics Chalmers University of Technology SE-412 96 Göteborg Sweden

E-mail: mpersson@liverpool.ac.uk

**Abstract.** We present a simplified density functional theory (DFT) method to compute vertical electron and hole attachment energies to frontier orbitals of molecules adsorbed on insulating films supported by a metal substrate. The adsorbate and the film is treated fully within DFT, whereas the metal is treated implicitly by a perfect conductor model. As illustrated for a pentacene molecule adsorbed on NaCl films supported by a Cu substrate, we find that the computed energy gap between the highest and lowest occupied molecular orbitals - HOMO and LUMO - from the vertical attachment energies increases with the thickness of the insulating film, in agreement with experiments. This increase of the gap can be rationalized in a simple dielectric model with parameters determined from DFT calculations and is found to be dominated by the image interaction with the metal. However, this model overestimates the downward shift of the energy gap in the limit of an infinitely thick film. This work provides a new and efficient strategy to extend the use of density functional theory to the study of charging and discharging of large molecular adsorbates on insulating films supported by a metal substrate.

Keywords: insulating film, metal substrate, adsorbates, charged system, frontier molecular orbitals, density functional theory

PACS numbers: 68.37.Ef 73.20.Mf 73.22.-f

## 1. Introduction

A remarkable capability of scanning probe microscopy is the possibility to form and control different (meta-)stable charged states of single atoms and molecules adsorbed on thin insulating films supported by a metal substrate [1–17]. These charged states can be manipulated and characterized on the atomic scale by scanning tunnelling microscopy (STM) [1–9] atomic force microscopy (AFM) [7–16] and Kelvin probe force microscopy (KPFM) [16, 17]. Charged states in molecular adsorbates are formed either by electron attachment to the lowest unoccupied molecular orbital (LUMO) or hole attachment to the highest occupied molecular orbital (HOMO) [3]. Control over the occupancy of frontier molecular states is crucial to alter selectively the catalytic properties of single adsorbates. Such a capability plays a decisive role in the field of molecular electronics, for example, where the ultimate goal is to use single molecules as functional building blocks for switches, rectifiers, transistors and memory [3–5, 14, 18–25]

Charge states of adsorbates can be stabilised either by having a sufficiently large polarization of the ionic film and the metal substrate or a sufficiently long lifetime using a sufficiently thick film to increase their life time. For example, the Au anion adsorbed on a NaCl bilayer is stabilized by the large polarization of the ionic film and the metal substrate [1], whereas in the case of a pentacene molecule adsorbed on this bilayer, this polarization is neither sufficiently large to stabilize the anion or the cation [3]. In contrast, for pentacene molecule on NaCl films thicker than 13 monolayers (ML), the electron transfer through the film is quenched and the life time is sufficiently

large so that both the cation and the anion become stable on the time scale of the experiments [14]. Nevertheless, the energies of frontier molecular orbitals is found to depend on film thickness. In fact, scanning tunneling spectroscopy of ultra-thin films ( $\leq 3\text{ML}$ ) and AFM experiments of thick films ( $> 20\text{ML}$ ) showed that the HOMO-LUMO gap of adsorbed pentacene increases with increasing the film thickness, but this gap was always smaller than its value in gas phase. This behaviour calls for calculations to gain a deeper insight into the interplay between metal substrate and film thickness in determining the energies of the frontier orbitals of the molecular adsorbates.

In principle, the electron and hole attachment energies which determine, for instance, the observed HOMO-LUMO gap of molecular adsorbates cannot simply be computed using ground state density functional theory (DFT) [26, 27], and an excited-state theory such as the GW approximation is required [28]. However, GW calculations are very expensive for typical molecular adsorbates [29] and have so far only been applied to a CO molecule adsorbed on NaCl films supported by a semi-conductor [30].

For adsorbates on thin insulating films supported by a metal substrate even the computation of ground state energies for stable charged states can be very challenging at the DFT level [1, 2, 5] due to the charge-delocalisation error introduced by current exchange-correlation functionals [31, 32]. This error often leads to fractional charging, which problem can sometimes be eliminated using a DFT+U approach [33, 34]. This approach has been successfully applied to the calculation of multiply charged states of Ag adatoms [2].

A simplifying feature of this class of system is the insulating character of the ionic film, which significantly reduces the coupling of the adsorbate electronic states with the metal electronic states, and forms the basis for approximate schemes [35]. This weak coupling was considered previously in DFT calculations of electron attachment energies to vacancy states in a NaCl bilayer on a Cu surface by constraining the vacancy state to be occupied [16]. Recently, we developed an approximate method where the metal electrons are eliminated completely but the ionic film and the adsorbate are treated fully within DFT [36, 37]. The metal is simply replaced by a perfect conductor (PC) model and the remaining non-Hartree interactions between the metal substrate and the film are modelled by a simple force field (FF) whose parameters are obtained from full DFT calculations of the ionic film supported by the metal substrate. By construction, this new method (DFT-PC-FF) makes it possible to control the charge state of the adsorbate with a large reduction of the computational time. This method was applied successfully to the calculation of the Au anion on a NaCl bilayer supported by a Cu substrate [37].

In this work, we show how DFT-PC-FF simulations can be used to compute the energies of frontier molecular orbitals of adsorbates on insulating films supported by a metal substrate. As an example, we consider pentacene adsorbed on NaCl films of different thicknesses which are supported by a Cu substrate. In agreement with experiments, we find that the HOMO-LUMO gap increases with increasing number of NaCl layers. In addition, our findings are compared with the results from a simple

dielectric model of the adsorbed film with abrupt interfaces. We show that this simplified model is able to semi-quantitatively describe the variation of the HOMO-LUMO gap with film thickness but has also some shortcomings.

The paper is organised as follows. In Section 2 we describe the main ingredients of the DFT-PC-FF method and its application to the calculation of electron and hole attachment energies to an adsorbed molecule and the corresponding HOMO-LUMO gap. Computational details are presented in Sec. 3. Results for the electronic structure and the HOMO-LUMO energy gap for the isolated molecule are presented in Section 4.1. Results for the variation of this energy gap of an adsorbed pentacene molecule on NaCl films with the number of layers are presented and compared with experiments in Section 4.2. In this latter section we also compare the calculated and experimental energy gaps with the results from a simple dielectric model in order to elucidate the contributions from the film and the metal substrate. Finally, some concluding remarks of this work are presented in Section 5. Electrostatic units are used throughout in this paper.

## 2. Computation of charged states of adsorbates with DFT-PC-FF

The DFT-PC-FF method for the calculations of charged adsorbates on an ionic insulating film supported by a metal substrate has been described in detail in our previous work [36, 37]. Here, we just summarise the key points of this method and how it can be used to calculate the electron and hole attachment energies to an adsorbed molecule and the corresponding HOMO-LUMO gap.

In the DFT-PC-FF method, the electrons of the metal substrate are not explicitly included in the calculation but their screening is accounted for in a perfect conductor (PC) model. The residual non-Hartree interactions between the film and metal substrate are described by a force field (FF). The system is represented in a supercell with a prescribed total charge  $Q_s$  of the adsorbate and film, which is compensated by an induced charge  $-Q_s$  in the PC, so that the supercell is neutral. The total energy  $E_{PC-FF}^{(Q_s/e)}$  of the system is then given in this method by minimising the following energy functional

$$E_{PC-FF}^{(N_s)}[n_s] = \bar{E}_{PC}[n_s] - \frac{Q_s}{e}\Phi_{PC} + \sum_{k \in \text{FL}} \phi_k(z_k) \quad (1)$$

with respect to the electron density  $n_s$  of the adsorbate and the film under the constraint that the total charge of the electrons and the ions is  $Q_s$ . Here,  $\bar{E}_{PC}[n_s]$  is the energy functional of the adsorbate and the film system interacting with the PC and  $\Phi_{PC}$  is the effective work function. As detailed in Ref. [37], the difference between  $\Phi_{PC}$  and the workfunction  $\Phi$  of the film supported by the explicit metal substrate (with no adsorbate) is due to the overlap of the electron density of the film with the image plane in the PC model. This overlap gives rise to a potential difference between the PC plane and the vacuum level. The residual non-Hartree interactions between the film and metal substrate are described by a simple force-field (FF) based on non-polarisable pair potentials,  $\phi_k(z_k)$  which only depends on the perpendicular distance  $z_k$  between

the ions  $k$  in the first layer of the film and the image plane. Besides the atom kinds of the adsorbate and the films, the material specific parameters in the DFT-PC-FF method are the position  $z_{\text{im}}$  of the image plane in the PC model with respect to the metal surface plane, the effective work function  $\Phi_{\text{PC}}$  and the pair potentials in the FF. How these parameters were determined is described in Section 3.

In scanning tunneling spectroscopy and AFM experiments, the bias voltages corresponding to attaching a tunneling electron or hole to the adsorbate are determined by the transition energies  $\Delta E_e$  and  $\Delta E_h$  for attaching an electron or a hole from the Fermi level to the adsorbate at fixed ion-core positions, respectively. In the DFT-PC-FF method these energies are approximated by the following vertical transition energies

$$\Delta E_e = E_{\text{PC-FF}}^{(Q_s^0/e-1)} - E_{\text{PC-FF}}^{(Q_s^0/e)} \quad (2)$$

$$\Delta E_h = E_{\text{PC-FF}}^{(Q_s^0/e+1)} - E_{\text{PC-FF}}^{(N_s^0/e)}, \quad (3)$$

where the energies of the negatively charged state  $Q_s^0 - e$  and positively charged state  $Q_s^0 + e$  are obtained at the calculated equilibrium geometry for the molecule in its ground state with charge  $Q_s^0$ . Note that in the presence of a metal support these charge states are not electronic ground states but are resonances due to mixing with metallic states. However, this mixing is already very weak, for instance, for a pentacene molecule adsorbed on a NaCl bilayer due to its insulating character, resulting in very narrow resonances with an estimated broadening of a few hundreds of an  $\mu\text{eV}$  [1]. Thus, the ground state energies obtained by neglecting this mixing should be an excellent approximation to these resonance energies. Since the system is represented in a supercell, the computed results are expected to depend on the surface area or coverage due to electrostatic adsorbate-adsorbate interactions. Thus, it is necessary to correct  $\Delta E_e$  and  $\Delta E_h$  for the dipole-dipole interactions between periodic images, as described in Appendix A.

If the adsorbed molecule is neutral ( $Q_s^0 = 0$ ) as for the adsorbed pentacene molecule then the HOMO-LUMO gap can be obtained from the vertical transition energies  $\Delta E_e$  and  $\Delta E_h$  as follows

$$E_G = \Delta E_e + \Delta E_h = E_{\text{PC-FF}}^{(-1)} + E_{\text{PC-FF}}^{(+1)} - 2E_{\text{PC-FF}}^{(0)}. \quad (4)$$

Note that this result for  $E_G$  is independent of the (effective) work function  $\Phi_{\text{PC}}$  of the metal and the film. For a reference, the corresponding HOMO-LUMO gap for an isolated neutral molecule,  $E_{G0}$ , was also calculated from the vertical affinity  $A = E^{(0)} - E^{(-1)}$  and ionisation energies  $I = E^{(+1)} - E^{(0)}$  as

$$E_{G0} = I - A = E^{(+1)} + E^{(-1)} - 2E^{(0)} \quad (5)$$

where  $E^{(Q/e)}$  is the total energy of the isolated molecule with a net charge of  $Q$  in the equilibrium geometry of the neutral molecule.

### 3. Computational details

Periodic DFT calculations were performed using the VASP code [38, 39]. All the required modifications for the implementation of the DFT-PC-FF method in VASP

have already been detailed in Refs. [36] and [37]. The projector augmented wave method (PAW) [40, 41] was used to describe the electron-ion interaction with a plane wave cut-off energy of 400 eV. The electronic exchange and correlation effects were treated using the optB86b-vdW version of the van der Waals (vdW) density functional [42, 43]. The NaCl bilayer supported by a Cu(100) substrate was modelled using a slab in a supercell. As detailed in Ref. [37], each primitive surface unit cell was composed of four layers of Cu atoms with nine Cu atoms in each layer, and a NaCl film that contained four atoms of each species in each layer. Note that in the DFT-PC-FF simulations this unit cell only contained the eight atoms of the NaCl film.

The Cu substrate was included explicitly just to compute the pentacene molecule adsorbed on a NaCl bilayer in order to make a comparison with the DFT-PC-FF results. We shall refer to this calculation as DFT-full. In this calculation, the supercell included  $3 \times 2$  repetitions of the primitive surface unit cell.

In the DFT-PC-FF method, the dependence on the lateral size of the supercell was investigated for the NaCl bilayer using supercells containing  $3 \times 2$ ,  $3 \times 3$ ,  $4 \times 3$  and  $4 \times 4$  repetitions of the primitive surface unit cell. In the case of NaCl films thicker than the bilayer only supercells containing the  $4 \times 3$  surface unit cells were considered. The lateral sizes of the supercells were sufficiently large to limit the sampling of the surface Brillouin zone to the  $\Gamma$ -point. All ionic relaxations were carried out with a convergence criteria of 0.02 meV/Å for the magnitude of the forces. The density of states of partial waves (PDOS) around the various atom sites were obtained using the PAW method.

As reported in Ref. [37] for the Cu(100) substrate, the value of 1.48 Å for  $z_{\text{im}}$  was obtained from the calculated response of this substrate to an external electric field. A value of 3.24 eV for  $\Phi_{\text{PC}}$  was obtained from the calculated electrostatic potential and  $\Phi = 3.74$  eV was the computed work function of the supported NaCl bilayer including the Cu(100) substrate in the DFT-full simulation. Furthermore, the functional form and the parameters of the pair potentials are the same as for the non-polarisable FF developed in Ref. [37], which were obtained from DFT calculations of the NaCl bilayer on the Cu(100) substrate.

In order to calculate  $E_{\text{G0}}$  from Eq. (5 of the isolated pentacene molecule), spin-polarized calculations using the Makov-Payne scheme [44] were performed for a positively and negatively charged molecule in a cubic supercell. Total energies including dipole corrections were converged for a supercell with a side length of 30 Å.

## 4. Results

In this section, we present the results of the DFT-PC-FF simulations for the vertical transition energies  $\Delta E_e$  and  $\Delta E_h$  and the corresponding HOMO-LUMO gap,  $E_G$ , for a single pentacene molecule adsorbed on NaCl films with different number of atomic layers. Computed energies are compared with experimental results. In addition, we present and discuss results for a simplified electrostatic model of this system. We begin by addressing the problem of an isolated pentacene molecule in vacuum.

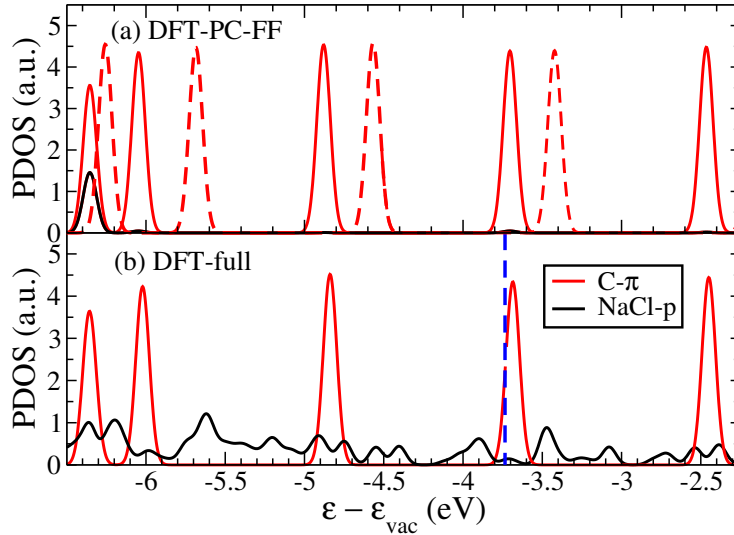


**Figure 1.** (online color) Calculated PDOS of  $p$  partial waves around the Na and Cl ions (solid black lines) and  $p_z$  partial waves around all C atoms of an isolated pentacene molecule (dashed red lines) and a pentacene molecule adsorbed on a NaCl bilayer supported by a Cu(100) substrate (red lines) using (a) DFT-PC-FF and (b) DFT-full. All energies are referenced with respect to the vacuum level  $\epsilon_{\text{vac}}$ . The Fermi energy in (b) is indicated by the vertical dashed blue line. The PDOS was broadened by a Gaussian with a broadening (FWHM) of 0.1 eV.

#### 4.1. Isolated pentacene molecule

As a reference case, the electronic states and the HOMO-LUMO gap  $E_{\text{G0}}$  of the isolated pentacene molecule were also computed. The energies of the  $\pi$  orbitals of the molecule were revealed by the calculated PDOS of  $p_z$  states of all C atoms of the neutral molecule, as shown by the dashed red lines in Fig. 1(a). The calculated orbital densities of the frontier orbitals – HOMO and LUMO – which are of  $\pi$  character are shown in the upper panel of Fig. 2. As expected from DFT calculations using a GGA-like approximation like the optB86b-vdW for the exchange-correlation functional, the calculated band gap from the computed Kohn-Sham (KS) energies of the HOMO and LUMO is 1.14 eV, which severely underestimates the experimental value of 5.27 eV [3, 45]. In contrast, DFT calculations of the total energies of the positively and negatively charged, as well as the neutral molecule in the equilibrium geometry of the neutral molecule, as detailed in Sec.3 and using Eq. (5), gave a much improved value of  $E_{\text{G0}} = 4.62$  eV. This result is in good agreement with the value of 4.73 eV from previous DFT calculations using the PBE functional [46], and the result of 4.72 eV from time-dependent DFT calculations using the B3LYP functional [47].

#### 4.2. Pentacene adsorbed on the NaCl bilayer supported by a Cu(100) surface

DFT-full calculations show that the adsorbed molecule on the NaCl bilayer supported by the Cu(100) surface is neutral and preserves the planar geometry [48] of the isolated

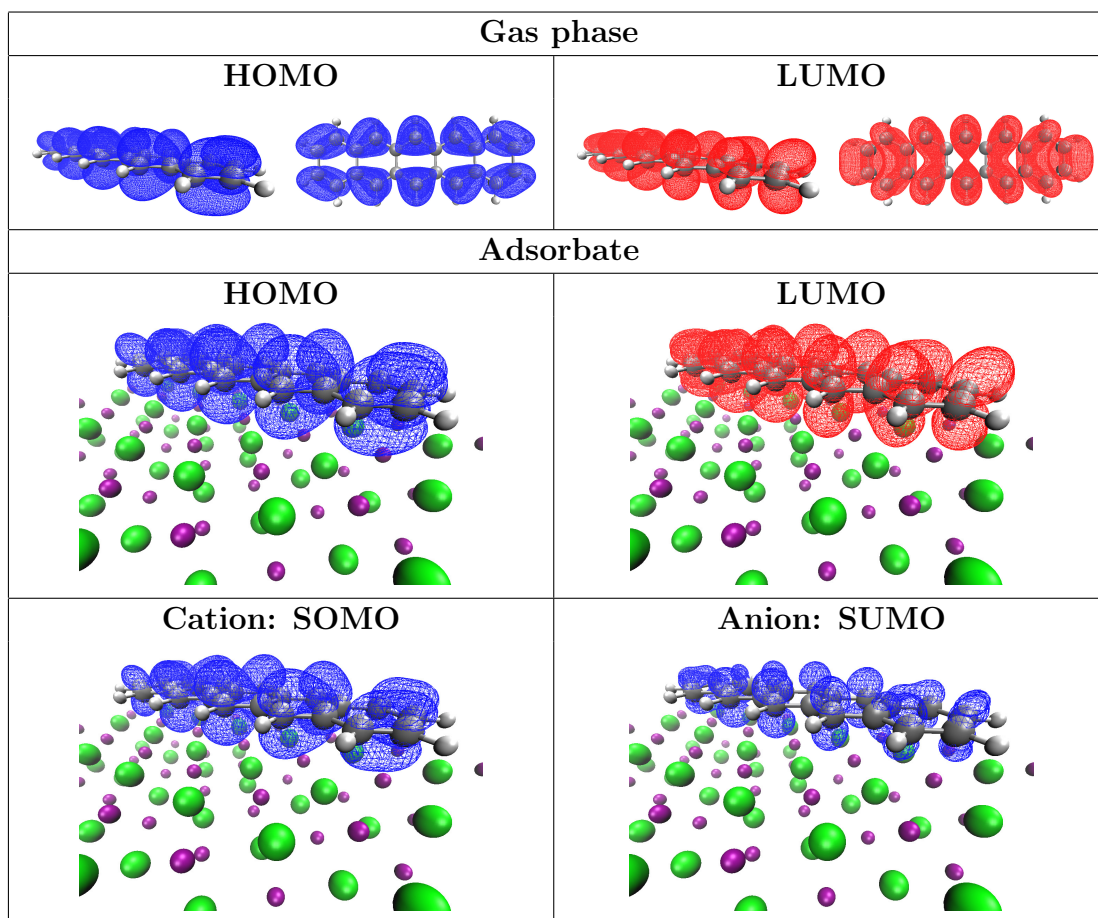


**Figure 2.** (online colour) Iso-surfaces of the electron densities of the frontier orbitals of the neutral isolated (upper panel) and adsorbed (middle panel) pentacene molecule, and of the negatively and positively charged adsorbed pentacene molecule (lower panel). Results of middle and lower panel were computed with the DFT-PC-FF method. Isosurfaces are taken at  $5 \times 10^{-3} \text{ e}/\text{\AA}^3$ . The C and H atoms of pentacene and the Na and Cl ions are represented by grey, white, violet and green spheres, respectively.

free molecule with negligible changes in the interatomic distances. In the most stable configuration of the adsorbed molecule, the central aromatic ring is on top of a Cl anion with a distance of 3.05 Å from the outermost NaCl layer. This large distance and the rather weak adsorption energy of 1.65 eV is due to the closed-shell electronic structure of pentacene and the formation of a physisorption bond. Results obtained using the DFT-PC-FF calculations give a very similar molecule-surface distance of 3.06 Å and an adsorption energy of 1.68 eV. This good agreement provides strong support for our proposed DFT-PC-FF method, especially considering also the massive reduction of the computational time by a factor of about 70 compared to the DFT-full calculations.

The electronic structure of adsorbed pentacene was analysed using the PDOS of the  $C-p_z$  states of pentacene (the  $\pi$  orbitals) and the  $p$  states of the ions in the NaCl bilayer. Results for DFT-FF-PC and DFT-full are shown in Fig. 1(a) and (b), respectively. In addition,  $C-p_z$  states of isolated pentacene are shown in Fig. 1(a) as a reference.



A comparison between the PDOS of the DFT-full calculations of adsorbed pentacene and the DFT calculations of isolated pentacene show that there is no discernible broadening of the  $\pi$  orbitals due to their interaction with the states of the film and the substrate. In addition, the  $\pi$  orbitals of adsorbed pentacene, except the orbital around -6.35 eV, experience only a small rigid downward shift of about 0.30 eV with respect to the vacuum level. The smaller shift of the orbital at -6.35 eV is due to its interaction with  $p$  states of the ions in the film. The DFT-full results show that the HOMO level is 1.09 eV below the Fermi energy ( $\varepsilon_F$ ), whereas the LUMO is just above  $\varepsilon_F$ . Finally, the PDOS of the  $p$  states of the ions NaCl in the bilayer shows up as a broad distribution, which is a result of their interaction with the Cu substrate states.

A comparison between the upper and middle panels of Fig.2 show that the electron densities of the HOMO and the LUMO of the adsorbed neutral molecule computed with DFT-PC-FF are very similar to the corresponding orbital densities of the isolated molecule and exhibit the same nodal structure. In addition, the difference between the KS energies gives a HOMO-LUMO gap of 1.17 eV, which is very close to the corresponding KS value of 1.14 eV for the isolated molecule. From Fig. 1, one finds that the  $p_z$  states of all the C atoms using the DFT-PC-FF method are in excellent agreement with the DFT-full results obtained by the explicit inclusion of the Cu(100) substrate. This agreement shows that the mixing of the  $\pi$  orbitals with Cu states are negligible and provides further support to the application of the DFT-PC-FF method to this system.

### *4.3. Frontier orbitals energy gaps and ionic resonances*

The anion and cation states of the adsorbed pentacene molecule on the NaCl(2ML)/Cu(100) were calculated using the DFT-PC-FF method by adding a single electron or hole to the neutral adsorbed pentacene on the NaCl bilayer at a fixed geometry corresponding to the calculated equilibrium geometry of the neutral molecule and film. Since the charging and discharging results in an odd number of electrons, spin polarisation was included in the simulations. The characters of the highest occupied orbitals following charging and discharging are demonstrated by the calculated orbital densities in lower panel of Fig. 2. These densities correspond to a singly occupied molecular orbital (SOMO) and a single unoccupied molecular orbital (SUMO) for the cation and the anion, respectively, which are very similar in shape to the LUMO and HOMO of the isolated and adsorbed molecule, respectively.

In the case of an adsorbed pentacene on a NaCl bilayer, Fig. 3 shows the calculated vertical electron and hole attachment energies  $\Delta E_e$  and  $\Delta E_h$  for different lateral sizes of the supercell or coverage, as obtained from Eq.(2) and (3). Here, the effective lateral size is defined by  $L_{\text{eff}} = \sqrt{L_x L_y}$  where  $L_x$  and  $L_y$  are the lengths of the supercell along  $x$  and  $y$  directions, respectively. Due to long-range electrostatic interactions between the periodic replica of the adsorbed molecule,  $\Delta E_e$  and  $\Delta E_h$  converge slowly with increasing  $L_{\text{eff}}$  to their zero-coverage values of a single adsorbed molecule. An extrapolation of  $\Delta E_e$

and  $\Delta E_h$  to the zero-coverage limit is done here by subtracting the dominant long-range electrostatic interaction, the dipole-dipole interaction, between the periodic replica, as detailed in Appendix A. This dipole correction improve considerably the convergence to the zero-coverage limit, as shown by the dipole-corrected energies  $\Delta E_e$  and  $\Delta E_h$  in Fig. 3. Note that the corresponding dipole-dipole interactions in the perpendicular  $z$  direction are already cancelled by the dipole correction provided by the dipole layer in the vacuum region [36,37]. Using the dipole-corrected energies we obtain zero-coverage values of 2.06 and 0.95 eV for  $\Delta E_e$  and  $\Delta E_h$ , respectively. The corresponding HOMO-LUMO gap  $E_G$ , as obtained directly from  $\Delta E_e$  and  $\Delta E_h$  using Eq. (4), is equal to 3.01 eV. This value is substantially larger than the value of 1.17 eV obtained from the calculated KS energies for the HOMO and the LUMO of the neutral adsorbed molecule. Interestingly, the value of 3.01 eV is a bit less than the the calculated value of 4.62 eV of  $E_G$  for the isolated molecule. We attribute this difference to the electronic polarisation of the positively and negatively charged molecule by the NaCl film.

The calculated vertical electron and hole attachment energies can be compared with the experimental energies for the positive and negative ionic resonances (NIR and PIR) by scanning tunneling spectroscopy of a single pentacene molecule adsorbed on NaCl films supported by a Cu(100) substrate [3]. A comparison of STM images at the biases of the NIR and PIR with computed images showed that these resonances correspond to electron and hole attachment from the tip to the LUMO and HOMO of the molecule, respectively. The observed values of 1.3 and -2.8 V for the sample biases of the NIR and PIR, respectively, give  $\Delta E_e = 1.3$  eV and  $\Delta E_h = 2.8$  eV and a value of 4.1 eV for  $E_G$ . Thus, the experimental value of  $E_G$  is reduced by approximately 1.17 eV upon adsorption on the bilayer. Surprisingly, the deviation of about 1.09 eV between the experimental (4.1 eV) and computed value (3.01 eV) for  $E_G$  is somewhat a bit larger than the corresponding deviation of 0.65 eV for the isolated molecule in vacuum (5.27 eV and 4.62 eV for experimental and computed  $E_G^0$ , respectively, as reported in section 4.1).

Here, the effect of the NaCl film on  $E_G$  was investigated by calculating  $E_G$  as a function of the number of monolayers  $N_l$  of the film. In these calculations, the values of  $E_G$  from 2 to 5 ML were obtained from the dipole-corrected  $\Delta E_e$  and  $\Delta E_h$  for a supercell with  $4 \times 3$  surface unit cell (see Section 3) corresponding to  $L_{eff} \approx 26.5$  Å. Computed values of  $E_G$  as a function of  $1/N_l$  are shown in Fig.4 (a), . In addition, we have included the calculated gap from the KS energies as well as the experimental values. For comparison, we also show in dashed lines computed and experimental values of the isolated molecule.

The observed increase of  $E_G$  with increasing  $N_l$  is reproduced by calculated values. In particular, the observed experimental reduction of about 0.3 eV for  $E_G$  between the bilayer ( $1/N_l = 1/2$ ) and the trilayer ( $1/N_l = 1/3$ ) is rather well reproduced by the calculated reduction of 0.22 eV.

The increase of  $E_G$  with the  $N_l$  can be understood in a simple dielectric model from the screening by the metal substrate and the film, as detailed in Appendix B. The metal

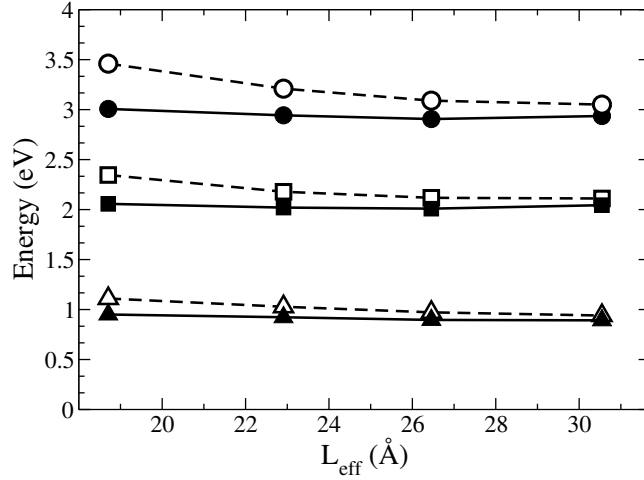


**Figure 3.** Calculated electron (diamonds) and hole (squares) attachment energies and HOMO-LUMO energy gaps (circles) for the adsorbed pentacene molecule as a function of the effective lateral size of the NaCl bilayer  $L_{\text{eff}}$ . Due to the electrostatic interaction between the infinite replica, computed values clearly decrease with  $L_{\text{eff}}$  towards limiting value for zero coverage (empty symbols). By substrating the dipole energy correction of Appendix A, convergence to the zero coverage limit is much improved (filled symbols).

is modelled by a perfect conductor, whereas the film is modelled by an homogeneous dielectric with an effective thickness  $a(N_1)$  and electronic dielectric constant  $\epsilon_\infty$  (see Fig. B1). The values of these parameters and the distance  $z_d - z_s$  between the dielectric vacuum interface and the average NaCl surface layer position  $z_s$  were determined by applying an homogeneous external electric field to the adsorbed film, as detailed in Appendix C. The electronic dielectric constant  $\epsilon_\infty$  and  $z_d - z_s$  were both found to be essentially independent of  $N_1$  with  $\epsilon_\infty \approx 2.64$  and  $z_d - z_s \approx 1.66$  Å, while the effective thickness of the film was well-approximated by  $a(N_1) \approx a_0 + N_1 \Delta a$  for  $N_1 = 2 - 5$  where  $a_0 \approx 0.84$  Å and  $\Delta a \approx 2.81$  Å. The value for  $\Delta a$  is essentially equal to the interlayer distance. In addition, the lateral extension of the surface charge distribution  $\sigma_{\text{ext}}(\mathbf{R})$  of the positively and negatively charged molecule has simply been modelled as an homogeneously charged rectangular sheet with a net charge of  $\pm e$ . The values for the side lengths  $D_x = 14.1$  Å and  $D_y = 5.0$  Å of the sheet were simply determined from the length and width of the pentacene molecule.

In this model, the layer dependence of the energy difference  $\Delta E_G(N_1)$  between the energy gap for the adsorbed and isolated molecule is given by (See Appendix B)

$$\begin{aligned} \Delta E_G(N_1) &= E_G(N_1) - E_{G0} \\ &= - \int \int \frac{d^2 K (\epsilon_\infty - 1) \exp(2Ka(N_1)) + (\epsilon_\infty + 1)}{2\pi K (\epsilon_\infty + 1) \exp(2Ka(N_1)) + (\epsilon_\infty - 1)} |\sigma_{\text{ext}}(\mathbf{K})|^2 \exp(-2KD) \end{aligned} \quad (6)$$

where  $D$  is the distance of the molecule from the dielectric-vacuum interface and the lateral Fourier transform of the charged sheet  $\sigma_{\text{ext}}(\mathbf{K})$  is given by Eq.(B.6). Here,  $D$  is determined from the calculated equilibrium distance  $d = 3.06$  Å of the molecule from the outermost NaCl layer, as  $D = d - z_d + z_s = 1.36$  Å. The resulting  $\Delta E_G(N_1)$  is shown

in Fig. 4(b). A better understanding of the  $N_1$  dependence  $\Delta E_G(N_1)$  in this model is obtained from an asymptotic expansion for large  $N_1$ , which is given by (see, Appendix B),

$$\Delta E_G(N_1) \asymp -\frac{\epsilon_\infty - 1}{2(\epsilon_\infty + 1)} \frac{\tilde{Q}_F^2}{D} - \frac{4\epsilon_\infty}{2(\epsilon_\infty + 1)^2} \frac{\tilde{Q}_M^2}{D + N_1 a}, \quad N_1 \rightarrow \infty. \quad (7)$$

Here, the effective charges  $\tilde{Q}_{F,M}$  take into account the lateral extension of the charge distribution of the charged molecule and are defined in Eq. (B.8). In the case of a point charge with charge  $\pm e$ ,  $\tilde{Q}_F^2 = \tilde{Q}_M^2 = e^2$  but  $\tilde{Q}_{F,M}$  decreases for an increasing lateral extension of the charge distribution. In the case of our simple model for the charge distribution of the HOMO and LUMO of pentacene the reduction is quite substantial  $\tilde{Q}_F^2 = 0.53e^2$  and but much less so for  $\tilde{Q}_M^2 = 0.92 - 0.96e^2$  due to the much larger distance of the molecule from the metal surface than its distance from the dielectric film. The leading order term on the right hand side of Eq. (7) gives the energy gap  $\Delta E_G(N_1 \rightarrow \infty)$  of the molecule adsorbed on a bulk dielectric, whereas the second term gives the contribution to  $E_G(N_1)$  from the image interaction with the metal surface screened by the dielectric film. The asymptotic result in Eq.(7) for  $E_G(N_1)$  is also shown in in Fig. 4 (b) and is close to the full result from Eq. (7). Here, we have also illustrated that the dielectric screening of the image interaction with the metal gives rise to relatively small reduction of  $\frac{(\epsilon_\infty+1)^2}{4\epsilon_\infty} \approx 1.25$  in this case by showing the corresponding result for the unscreened image interaction with the surface.

As shown in Fig. 4 (b), from a comparison of the results of the dielectric model for  $\Delta E_G(N_1)$  with the calculated results using DFT-PC-FF, the bulk limit of  $\Delta E_G(N_1 \rightarrow \infty)$  is severely overestimated by the dielectric model. The dielectric model gives a value of -1.25 eV in this limit for  $\Delta E_G(N_1)$  whereas an extrapolation of the calculated values to  $N_1 \rightarrow \infty$  gives a value of only about -0.58 eV for the downward shift. The corresponding extrapolated value from the experiments gives even a smaller downward shift of -0.28 eV. The significant overestimate of the downward shift in the bulk limit of  $\Delta E_G$  in the dielectric model demonstrates the challenges of modelling the response of an ionic insulating film to a charged adsorbate at a close distance where the electron density distributions of the dielectric film and the charged molecule are not well-separated. The variation of  $\Delta E_G$  obtained from DFT-PC-FF is better described with the dielectric model than the bulk limit  $\Delta E_G(N_1 \rightarrow \infty)$  but tends to underestimate the variation. A somewhat surprising behaviour of the measured  $\Delta E_G(N_1)$  is its near-linear behaviour even down to  $N_1 = 1$ , which is not really captured either by the DFT-PC-FF calculation or the dielectric model.

## 5. Summary and conclusions

In this work, we have addressed the problem of calculating electron and hole attachment energies of an adsorbed molecule, whose electronic states are essentially decoupled from the conduction electron states of the metal substrate by an insulating film. To this purpose, we have used our recently developed DFT-PC-FF method, where both the film

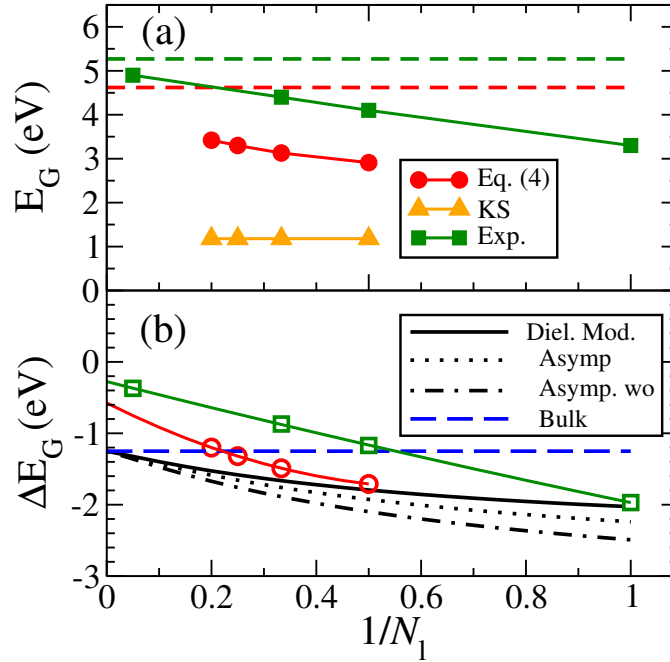


**Figure 4.** (online colour) (a) Calculated and experimental HOMO-LUMO energy gaps,  $E_G$ , for the adsorbed pentacene molecule and (b) its shift  $\Delta E_G$  with respect to its gas-phase value as a function of  $1/N_1$ , where  $N_1$  is the number of NaCl monolayers. The calculated  $E_G$  (solid circles) were obtained from DFT-PC-FF calculations of the negatively and positively charged molecules using Eq. (4), including lateral dipole corrections. (a)  $E_G$  obtained from the calculated Kohn-Sham energies are significantly underestimated (solid triangles). The experimental  $E_G$  (solid squares) were obtained from measurements by scanning tunneling spectroscopy [1] and atomic force microscopy [14]. The calculated and the experimental  $E_G$  of the isolated molecule are also indicated by red and green dashed lines, respectively. (b) The extrapolation of the calculated and the experimental values of  $\Delta E_G$  to  $N_1 \rightarrow \infty$  was obtained by a fit to a quadratic polynomial in  $1/N_1$ . We have also included the results for  $\Delta E_G$  in the dielectric model, Eq.(7), (solid line) and also its asymptotic result for  $\Delta E_G$ , Eq.(7), with (dotted line) and without (dot-dashed line) the dielectric screening of image interaction with the perfect conductor. The bulk limit of  $\Delta E_G$  in the dielectric model is indicated by the blue dashed line.

and the adsorbed molecule are treated fully within DFT, whereas the metal substrate is treated implicitly by a perfect conductor (PC) model. The remaining non-Hartree interactions between the metal substrate and the film are modelled by a simple force field (FF) whose parameters are obtained from DFT calculations.

As an example case, we have considered a pentacene molecule adsorbed on NaCl films supported by a Cu(100) surface and compared our results with scanning tunneling spectroscopy and atomic force microscopy experiments. Support for our method comes from the very good agreement of the DFT-PC-FF results for the relaxed geometry and adsorption energy of the adsorbed molecule on an NaCl bilayer supported by a Cu(100) surface with the results from our DFT calculations which include the metal substrate explicitly. The adsorbed molecule is found to be neutral and keeps the planar geometry

of gas phase. The molecule is physisorbed on the film as evidenced by the calculated PDOS which shows that the frontier orbitals experience only a small rigid shift in energy.

The calculated HOMO-LUMO energy gap for a fixed geometry increases with the number of NaCl layers in agreement with the experiments. The calculated energy gap underestimate somewhat the experimental gap, in part due to the underestimate of the observed gap of the isolated molecule by the used exchange-correlation energy functional. The calculated energy gap is much improved over the energy gap as obtained from the calculated KS energies for the HOMO and the LUMO.

The layer dependence of the calculated energy gap was analyzed in a simple dielectric model of the adsorbed film with parameters taken from DFT calculations of the response of the adsorbed film to an external electric field. This model rationalizes semi-quantitatively the observed behaviour of the energy gap with the number of layers and elucidates the contributions from the film and the metal substrate to the shift of the energy gap with the number of layers. In particular, this model reveals that the decrease of the energy gap with decreasing number of layers is primarily due to the electrostatic interaction with the metal. Nevertheless, values calculated with this model depart significantly from the experimental and the calculated DFT-PC-FF values. This highlights the challenges of building a proper electrostatic model of charged adsorbates on a insulating film.

## **Acknowledgments**

The authors acknowledge Leverhulme Trust for funding this project through the grant (F/00 025/AQ) and allocation of computer resources at HECToR through the membership in the materials chemistry consortium funded by EPSRC (EP/L000202F) and at Lindgren PDC through SNIC. We also thank Prof. Jasha Repp and Dr. Gerhard Meyer for useful input. Mats Persson is grateful for the support from the EU project ARTIST.

## **Appendix A. Dipole-dipole energy correction from the interaction between periodic images**

In periodic DFT calculations the adsorbate coverage is determined by the lateral size of the supercell. In order to study single adsorbates corresponding to the zero coverage limit one needs to perform calculations for increasing lateral sizes of the supercell in order to extrapolate the results to the limit of infinite lateral size or zero coverage. This task can be computationally very demanding due to the slow convergence caused by long-range electrostatic interactions of the adsorbate with its periodic images. The dipole-dipole interaction term is the leading order term of these interactions. Here we provide an explicit expression for lateral dipole-dipole energy correction in the PC model for charged adsorbates which significantly improves the convergence to the zero-coverage limit. Note that the perpendicular dipole-dipole interactions are already corrected for

by the introduction of a dipole layer in the vacuum region.

Following the notation introduced in Ref. [36] for the PC model  $\rho_s(\mathbf{r})$  is the charge density of the charged system that includes both the insulating film and the charged adsorbate inside a supercell  $V$  and  $\rho_{\text{ind}}(\mathbf{r})$  is the induced charge at the PC plane which is located at the image position  $z_{\text{im}}$  of the bare metal substrate. The resulting electrostatic potential  $\phi(\mathbf{r})$  has not only a contribution from  $\rho(\mathbf{r}) = \rho_s(\mathbf{r}) + \rho_{\text{ind}}(\mathbf{r})$  but also a contribution from a dipole layer  $\rho_{\text{dip}}(z)$  at a plane in the vacuum region which compensates for the perpendicular dipole-dipole interactions. The undetermined constant of  $\phi(\mathbf{r})$  is fixed by the condition that  $\phi(\mathbf{r}) = 0$  inside the metal. The corresponding charge density and electrostatic potential in the absence of the charged adsorbate is denoted by  $\rho_{s0}(\mathbf{r})$  and  $\phi_0(\mathbf{r})$  respectively. The change in electrostatic interaction energy upon adsorption is then given by

$$\begin{aligned} \Delta E_{\text{el}} &= \frac{1}{2} \int_V \rho_s(\mathbf{r}) \phi(\mathbf{r}) d^3r - \frac{1}{2} \int_V \rho_{s0}(\mathbf{r}) \phi_0(\mathbf{r}) d^3r & (\text{A.1}) \\ &= \frac{1}{2} \int_V \Delta\rho_s(\mathbf{r}) \phi_0(\mathbf{r}) d^3r + \frac{1}{2} \int_V \rho_{s0}(\mathbf{r}) \Delta\phi(\mathbf{r}) d^3r + \frac{1}{2} \int_V \Delta\rho_s(\mathbf{r}) \Delta\phi(\mathbf{r}) d^3r & (\text{A.2}) \end{aligned}$$

where  $V$  is the volume of the supercell  $\Delta\rho_s(\mathbf{r}) = \rho_s(\mathbf{r}) - \rho_{s0}(\mathbf{r})$  and  $\Delta\phi(\mathbf{r}) = \phi(\mathbf{r}) - \phi_0(\mathbf{r})$ . The first term in Eq. (A.2) is the electrostatic potential energy of the localized adsorbate-induced charge density  $\Delta\rho_s(\mathbf{r})$  in the potential  $\phi_0(\mathbf{r})$  and will be rapidly convergent with increasing lateral size of the supercell. The two remaining terms in Eq. (A.2) can be handled by introducing the electrostatic field  $\Delta\phi^{(0)}(\mathbf{r})$  from the charge distribution induced by the adsorbate in the zero-coverage limit

$$\Delta\phi^{(0)}(\mathbf{r}) = \int \frac{\Delta\rho(\mathbf{r}')}{|\mathbf{r} - \mathbf{r}'|} d^3r' . \quad (\text{A.3})$$

The potential  $\Delta\phi(\mathbf{r})$  can now be expressed in terms of  $\Delta\phi^{(0)}(\mathbf{r})$  as a sum over the lateral lattice vectors  $\mathbf{R}_{\parallel}$  as

$$\Delta\phi(\mathbf{r}) = \sum_{\mathbf{R}_{\parallel}} \Delta\phi^{(0)}(\mathbf{r} - \mathbf{R}_{\parallel}) . \quad (\text{A.4})$$

Note that it is sufficient to restrict the summation over  $\mathbf{R}_{\parallel}$  due to the inclusion of the dipole layer  $\rho_{\text{dip}}(z)$  in the supercell. Using this decomposition and the periodicity of  $\rho_{s0}(\mathbf{r})$  the second term in Eq. (A.2) is given by

$$\frac{1}{2} \int_V \rho_{s0}(\mathbf{r}) \Delta\phi(\mathbf{r}) d^3r = \frac{1}{2} \int_V \rho_{s0}(\mathbf{r}) \Delta\phi^{(0)}(\mathbf{r}) d^3r \quad (\text{A.5})$$

which is nothing else than its zero coverage limit. Thus only the third term on the RHS in Eq. (A.2) contains the long-range electrostatic interactions and is given in term of the decomposition in Eq. (A.4) as

$$\frac{1}{2} \int_V \Delta\rho_s(\mathbf{r}) \Delta\phi(\mathbf{r}) d^3r = \frac{1}{2} \sum_{\mathbf{R}_{\parallel}} \int_V \Delta\rho_s(\mathbf{r}) \Delta\phi^{(0)}(\mathbf{r} - \mathbf{R}_{\parallel}) d^3r \quad (\text{A.6})$$

The  $\mathbf{R}_{\parallel} = \mathbf{0}$  term converges rapidly to the zero-coverage limit and the remaining terms which are the electrostatic potentials from the periodic images can be approximated by a multipole expansion. The leading order term in this expansion of the electrostatic potential of the neutral charge distribution  $\Delta\rho(\mathbf{r})$  will be a dipole potential given by

$$\Delta\phi^{(0)}(\mathbf{r} - \mathbf{R}_{\parallel}) \simeq \frac{2\Delta\mu_z(z - z_{\text{im}})}{R_{\parallel}^3} . \quad (\text{A.7})$$

Note that the screening by the perfect conductor gives rise to a dipolar electrostatic field with an effective dipole moment which is twice as large as the dipole moment  $\Delta\mu_z$  of the adsorbate-induced charge distribution given by

$$\Delta\mu_z = \int_V z\Delta\rho(\mathbf{r})d^3r = \int_V (z - z_{\text{im}})\Delta\rho_s(\mathbf{r})d^3r . \quad (\text{A.8})$$

From Eqs.(A.6),(A.7) and (A.8) one obtains that the electrostatic interaction energy  $\Delta E'_{\text{el}}$  from the periodic images is given by

$$\Delta E'_{\text{el}} \simeq \Delta\mu_z^2 \sum_{\mathbf{R}_{\parallel} \neq \mathbf{0}} \frac{1}{R_{\parallel}^3} . \quad (\text{A.9})$$

This interaction energy is repulsive and should be subtracted from the calculated total energies in order to correct for the dipole-dipole interactions between the periodic images. The lattice sum in Eq. (A.9) can be readily evaluated numerically. For a supercell with a square lateral shape of side length  $L$  this interaction energy decays as  $L^{-3}$

Finally note that this result as applied to an external charge outside the PC differs from the result that would be obtained from Eqs. (59) (62) and (63) in Ref. [36] in one important aspect. The results in Eqs. (59) and (62) were obtained from the electrostatic potential  $\phi_{\text{ind}}(\mathbf{r})$  of  $\rho_{\text{ind}}(\mathbf{r})$  rather than from  $\phi(\mathbf{r})$  as done here. Thus the result in Ref. [36] contains a contribution that decays as  $L^{-1}$  as first pointed out by G. Makov and M. C. Payne [44].

## Appendix B. A simple dielectric model of the adsorbed film

Here, we will derive the interaction energy for an external surface charge distribution outside a dielectric film supported by a perfect conductor (PC) model of the metal substrate. In this model, the shift of the HOMO-LUMO energy gap from its value for an isolated molecule is then given by the sum of the corresponding electrostatic interaction energies of the charge distributions for both the positively and negatively charged molecule with the supported film. As illustrated schematically in Fig. B1, the metal is modelled by a PC and the adsorbed film by a homogeneous dielectric film with thickness  $a$  and dielectric constant  $\epsilon$ . Here we will use the notation  $\mathbf{r} = (\mathbf{R}, z)$ .

The interaction energy of an external surface charge distribution  $\sigma_{\text{ext}}(\mathbf{R})$  at a distance  $D$  from the dielectric film is given by,

$$E_{\text{int}} = -\frac{1}{2} \int \int \frac{d^2K}{2\pi K} r(K) |\sigma_{\text{ext}}(\mathbf{K})|^2 \exp(-2KD) \quad (\text{B.1})$$



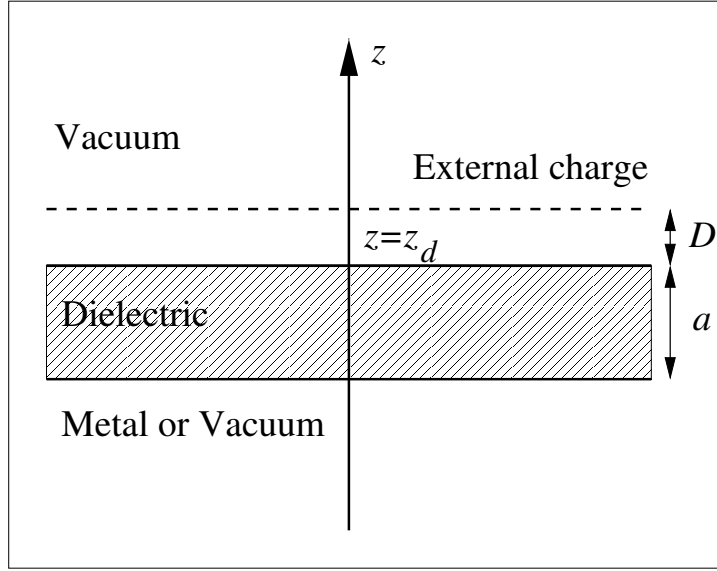


**Figure B1.** Schematics of the dielectric model of an adsorbed molecule on an ionic insulating film, which is either freestanding or supported by a perfect conductor model of the metal substrate. The dashed line indicates the position of the externally charged sheet.

where  $\sigma_{\text{ext}}(\mathbf{K})$  is the lateral Fourier transform of  $\sigma(\mathbf{R})$  and  $|\mathbf{K}| = K$ .  $r(K)$  is the reflection coefficient from the dielectric-vacuum interface at  $z = z_d$  of the evanescent plane wave component  $\phi_{\text{ext}}(\mathbf{K}) \exp(Kz)$  of the external electrostatic potential from  $\sigma_{\text{ext}}(\mathbf{R})$ . In the region  $z < z_d + D$ , the plane wave component  $\phi(z; \mathbf{K})$  of the electrostatic potential is then given by

$$\phi(z; \mathbf{K}) = \phi_{\text{ext}}(\mathbf{K}) \begin{cases} \exp(K(z - z_d)) - r(K) \exp(-K(z - z_d)) & z_d + D > z > z_d \\ t(K) \exp(K(z - z_d)) - s(k) \exp(-K(z - z_d)) & z_d > z > z_d - a \\ 0 & z_d - a > z \end{cases} \quad (\text{B.2})$$

The reflection coefficient  $r(K)$  and the coefficients  $s(K)$  and  $t(K)$  in Eq. (B.2) can now be determined from the boundary conditions that the parallel component of the electric field and the perpendicular component of the external electric field should be both continuous across the two interfaces. These boundary conditions gives,

$$r(K) = \frac{(\epsilon - 1) \exp(2Ka) + (\epsilon + 1)}{(\epsilon + 1) \exp(2Ka) + (\epsilon - 1)}. \quad (\text{B.3})$$

In the asymptotic limit of a thick dielectric film corresponding to  $a \rightarrow \infty$ ,  $r(K)$  in Eqns.(B.3) reduces to,

$$r(K) \asymp \frac{\epsilon - 1}{\epsilon + 1} + \frac{4\epsilon}{(\epsilon + 1)^2} \exp(-2Ka) \quad (\text{B.4})$$

Here we will go beyond the simple point charge model for the charge distribution of an adsorbed molecule with charge  $Q$  and take into account of the lateral extension of this

charge distribution by using the following simple rectangular surface charge distribution

$$\sigma_{\text{ext}}(\mathbf{R}) = \begin{cases} \frac{Q}{D_x D_y} |X| < \frac{D_x}{2} \text{ and } |Y| < \frac{D_y}{2} \\ 0 & \text{otherwise} \end{cases} \quad (\text{B.5})$$

whose Fourier transform is given by

$$\sigma_{\text{ext}}(\mathbf{K}) = \frac{4Q \sin\left(\frac{D_x K_x}{2}\right) \sin\left(\frac{D_y K_y}{2}\right)}{D_x K_x D_y K_y} \quad (\text{B.6})$$

The corresponding  $E_{\text{int}}$  are then readily calculated from Eqs.(B.1) thanks to the exponential decay of the integrand with  $K$  using a two-dimensional numerical quadrature .

The asymptotic interaction energy as obtained from  $r(K)$  in Eqs.(B.4) and (B.6) can now be expressed as,

$$E_{\text{int}} \asymp -\frac{\epsilon - 1}{4(\epsilon + 1)} \frac{Q^2}{D} - \frac{4\epsilon}{(\epsilon + 1)^2} \frac{Q^2}{4(D + a)}, \quad (\text{B.7})$$

where the effective charges  $\tilde{Q}_{F,M}$  are given by,

$$\tilde{Q}_{F,M}^2 = \int \int \frac{d^2 K}{2\pi K} |\sigma_{\text{ext}}(\mathbf{K})|^2 2h_{F,M} \exp(-2Kh_{F,M}). \quad (\text{B.8})$$

Here,  $h_F = D$  and  $h_M = D + a$  are the distances between the external charge and the surface of the dielectric film and the perfect conductor, respectively. Note that the first term in (B.7) is the interaction energy of the external charge distribution with a semi-infinite dielectric and the second term reduces to the corresponding interaction energy with a perfect conductor in the absence of the dielectric film  $\epsilon = 1$ . Thus the prefactor  $\frac{4\epsilon}{(\epsilon+1)^2}$  in the second term is due to the dielectric screening by the film.

### Appendix C. Determination of dielectric parameters for the adsorbed film

Here we show how the effective thickness  $a$  of the ionic insulating film and its effective electronic dielectric constant  $\epsilon_\infty$  were determined from the calculated response of the adsorbed film to an external homogeneous electric field  $\mathbf{E}_{\text{ext}} = E_{\text{ext}}\hat{z}$  for fixed nuclear positions. This electric field was included in our DFT-full and DFT-PC-FF calculations using the method described in Ref. [37]. Results for the induced electrostatic potentials  $\Delta\phi(z)$  are shown in Fig. C1 in the presence of a relatively weak external field of 0.05 eV/Å. The dielectric parameters were obtained by a least square fit of the calculated potentials to the induced electrostatic potential obtained in a dielectric model of the film and a perfect conductor model of the metal. Using standard electrostatics, one obtains the following potential across the dielectric film and the perfect conductor,

$$\Delta\phi(z) = -2E_{\text{ext}} \begin{cases} 0, & z < z_d - a \\ \frac{(z - z_d - a)}{\epsilon_\infty}, & z_d - a < z < z_d \\ (z - z_d + \frac{a}{\epsilon_\infty}), & z > z_d \end{cases} \quad (\text{C.1})$$

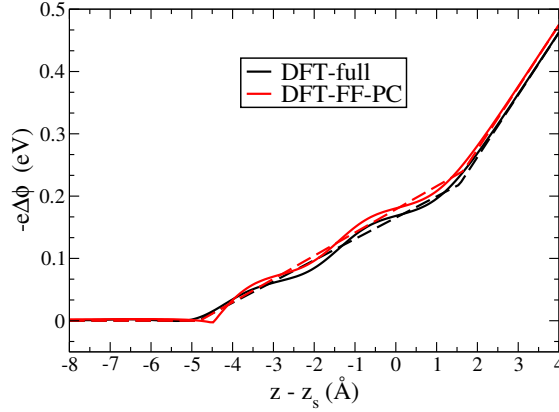


**Figure C1.** (online color) Calculated electrostatic potential energy induced by an external perpendicular homogeneous electric field across a NaCl bilayer supported by a Cu(100) surface as obtained by DFT (black solid line) and DFT-FF-PC (red solid line) for fixed nuclear positions. The dashed lines are corresponding least square fits to the dielectric model electrostatic potential in Eq. C.1.  $z_s$  is the position of the outermost NaCl plane. The strength of the external electric field is  $0.05 \text{ V/\AA}$ .

$N_1$	$\epsilon_\infty$	$a$ ( $\text{\AA}$ )	$z_d - z_s$ ( $\text{\AA}$ )
2	2.69	6.46	1.66
3	2.63	9.21	1.68
4	2.63	12.12	1.65
5	2.62	14.89	1.67

**Table C1.** Calculated dielectric model parameters for different numbers of NaCl layers  $N_1$  as obtained by a fit to the calculated response to an external electric field using DFT-FF-PC.  $z_d - z_s$  is the distance of the dielectric surface from the outermost surface plane.

This fit of the computed  $\Delta\phi(z)$  using DFT-full for the NaCl bilayer on the explicit Cu(100) surface to the model  $\Delta\phi(z)$  in Eq. C.1 gives  $\epsilon_\infty = 2.52$  and  $a = 6.26 \text{ \AA}$ . This fit using the results from DFT-PC-FF gives  $\epsilon_\infty = 2.69$  and  $a = 6.46 \text{ \AA}$ . In the case of a free-standing NaCl bilayer, a fit of a similar model potential for an free-standing dielectric film to the computed  $\Delta\phi(z)$  gives  $\epsilon_\infty = 2.5$  and  $a = 6.3 \text{ \AA}$ . This value of 2.5 for  $\epsilon_\infty$  is close to our calculated value of 2.47 for bulk NaCl using density functional perturbation theory method in VASP. Note that the value of  $6.3 \text{ \AA}$  for  $a$  is much larger than the distance of  $2.87 \text{ \AA}$  between the two layers of the free-standing bilayer. The corresponding results for  $N_1 = 3$  to 5 obtained by DFT-FF-PC are shown in Table C1 and the dielectric response of the film is well-represented by the average values of 2.64 and  $1.66 \text{ \AA}$  for  $\epsilon_\infty$  and  $z_d - z_s$ , respectively. Furthermore the layer dependence of  $a$  is well represented by  $a(N_1) \approx a_0 + N_1\Delta a$  for  $N_1 = 2$  to 5 where  $a_0 \approx 0.84 \text{ \AA}$  and  $\Delta a \approx 2.81 \text{ \AA}$ .

## References

- [1] Repp J, Meyer G, Olsson F E and Persson M 2004 Controlling the charge state of individual gold adatoms *Science* **305** 493
- [2] Olsson F E, Paavilainen S, Persson M, Repp J and Meyer G 2007 Multiple Charge States of Ag Atoms on Ultrathin NaCl Films *Phys. Rev. Lett.* **98** 176803
- [3] Repp J, Meyer G, Stojković S M, Gourdon A and Joachim C 2005 Molecules on Insulating Films: Scanning-Tunneling Microscopy Imaging of Individual Molecular Orbitals *Phys. Rev. Lett.* **94** 026803
- [4] Repp J, Meyer G, Paavilainen S, Olsson F E and Persson M 2006 Imaging bond formation between a gold atom and pentacene on an insulating surface *Science* **312** 1196
- [5] Mohn F, Repp J, Gross L, Meyer G, Dyer M S and Persson M 2010 Reversible Bond Formation in a Gold-Atom-Organic-Molecule Complex as a Molecular Switch *Phys. Rev. Letter* **105** 266102
- [6] Steurer W, Gross L and Meyer G. 2014 Local thickness determination of thin insulator films via localized states *Appl. Phys. Lett.* **104** 231606
- [7] Schuler B, Meyer G, Pena D, Mullins O C and Gross L 2015 Unraveling the Molecular Structures of Asphaltenes by Atomic Force Microscopy *J. Am. Chem. Soc.* **137** 9870-9876
- [8] Pavlicek N, Schuler B, Collazos S, Moll N, Perez D, Guitian E, Meyer G, Pena D and Gross L 2015 On-surface generation and imaging of arynes by atomic force microscopy *Nat. Chem.* **7** 623-628
- [9] Mohn F, Schuler B, Gross L and Meyer G 2013 Different tips for high-resolution atomic force microscopy and scanning tunneling microscopy of single molecules *Appl Phys. Lett.* **102** 073109
- [10] Moll N et al. 2014 Image Distortions of a Partially Fluorinated Hydrocarbon Molecule in Atomic Force Microscopy with Carbon Monoxide Terminated Tips *Nano Letters* **324** 6127-6131
- [11] Gross L, Mohn F, Liljeroth P, Repp J, Giessibl F J and Meyer G 2009 Measuring the Charge State of an Adatom with Noncontact Atomic Force Microscopy *Science* **324** 1428-1431
- [12] Majzik Z, Cuenca A B, Pavlicek N, Miralles N, Meyer G, Gross L and Fernandez E 2016 Synthesis of a Naphthodiazaborinine and Its Verification by Planarization with Atomic Force Microscopy *ACS Nano* **10** 5340-5345
- [13] Steurer W, Repp J, Gross L, Scivetti I, Persson M and Meyer G 2015 Manipulation of the Charge State of Single Au Atoms on Insulating Multilayer Films *Phys. Rev. Lett.* **114** 036801
- [14] Steurer W, Fatayer S, Gross L and Meyer G 2015 Probe-based measurement of lateral single-electron transfer between individual molecules *Nat. Comm.* **6** 8353
- [15] z Schuler B, Fatayer S, Mohn F, Moll N, Pavlicek N, Meyer G, Pena D and Gross L 2016 Reversible Bergman cyclization by atomic manipulation *Nat. Chem.* **8** 220-224
- [16] Gross L, Schuler B, Mohn F, Moll N, Pavlicek N, Steurer W, Scivetti I, Kotsis K, Persson M and Meyer G 2014 Investigating atomic contrast in atomic force microscopy and Kelvin probe force microscopy on ionic systems using functionalized tips *Phys. Rev. B* **90** 155455
- [17] Schuler B, Liu SX, Geng Y, Decurtins S, Meyer G and Gross L 2014 Contrast Formation in Kelvin Probe Force Microscopy of Single pi-Conjugated Molecules *Nano Letters* **14** 3342-3346
- [18] Liljeroth P, Repp J and Meyer G 2007 Current-induced hydrogen tautomerization and conductance switching of naphthalocyanine molecules *Science* **317** 1203-1206
- [19] Quek S Y, Kamenetska M, Steigerwald M L, Choi H J, Louie S G, Hybertsen M S, Neaton J B and Venkataraman L 2009 Mechanically controlled binary conductance switching of a single-molecule junction *Nat Nanotechnol* **4** 230-234
- [20] Diez-Perez I, Hihath J, Lee Y, Yu L, Adamska L, Kozhushner M A, Oleynik I I and Tao N 2009 Rectification and stability of a single molecular diode with controlled orientation *Nat Chem* **1** 635-641
- [21] Yee S K, Sun J, Darancet P, Tilley T D, Majumdar A, Neaton J B and Segalman R A 2011 Inverse rectification in donor-acceptor molecular heterojunctions *ACS Nano* **5** 9256-9263
- [22] Joachim C, Gimzewski J K and Aviram A 2000 Electronics using hybrid-molecular and mono-molecular devices *Nature* **408** 541-548

- [23] Lörtscher E 2013 Wiring molecules into circuits *Nat. Nanotechnol* **8** 381-384
- [24] Ratner M 2013 A brief history of molecular electronics *Nat., Nanotechnol* **8** 378-381
- [25] Schull G, Frederiksen T, Arnau A, Sanchez-Portal D and Berndt R 2011 Atomic-scale engineering of electrodes for single-molecule contacts *Nat. Nanotechnol* **6** 23-27
- [26] Hohenberg P and Kohn W Inhomogeneous Electron Gas 1964 *Phys. Rev.* **136** B864.
- [27] Kohn W and Sham L J Self-Consistent Equations Including Exchange and Correlation Effects 1965 *Phys. Rev.* **140** A1133
- [28] Aryasetiawan F and Gunnarsson O 1998 The GW method *Rep. Prog. Phys.* **61** 237
- [29] The GW method has been used to compute electronic excited states at a bcc(110) lithium surface, both bare and covered by ionic ultrathin (1-2 monolayers) LiF epitaxial films. See Sementa L, Marini A, Barcaro G, Negreiros F R and Fortunelli A Electronic excited states at ultrathin dielectric-metal interfaces 2013 *Phys. Rev. B* **88** 125413
- [30] Freysoldt C, Rinke P and Scheffler M Controlling Polarization at Insulating Surfaces: Quasiparticle Calculations for Molecules Adsorbed on Insulator Films 2009 *Phys. Rev. Lett.* **103** 056803
- [31] Godby R W, Schluter M and Sham L J Accurate Exchange-Correlation Potential for Silicon and Its Discontinuity on Addition of an Electron 1986 *Phys. Rev. Lett.* **56** 2415
- [32] Kim Y H and Görling A Exact Kohn-Sham exchange kernel for insulators and its long-wavelength behavior 2002 *Phys. Rev. B* **66** 035114
- [33] Anisimov V I, Zaanen J and Andersen O K Band theory and Mott insulators: Hubbard U instead of Stoner I 1991 *Phys. Rev. B* **44** 943
- [34] Cococcioni M and de Gironcoli S 2005 Linear response approach to the calculation of the effective interaction parameters in the LDA+U method 2005 *Phys. Rev. B* **71** 035105
- [35] Korventausta A, Paavilainen S, Niemi E and Nieminen J A STM simulation of molecules on ultrathin insulating overlayers using tight-binding: Au-pentacene on NaCl bilayer on Cu 2009 *Surf. Sci.* **603** 437-444
- [36] Scivetti I and Persson M The electrostatic interaction of an external charged system with a metal surface: a simplified density functional theory approach 2013 *J. Phys.: Condens. Matter* **25** 355006
- [37] Scivetti I and Persson M A simplified density functional theory method for investigating charged adsorbates on an ultrathin, insulating film supported by a metal substrate 2014 *J. Phys.: Condens. Matter* **26** 135003.
- [38] Kresse G and Furthmüller J Efficiency of ab-initio total energy calculations for metals and semiconductors using a plane-wave basis set 1996 *Comput. Mat. Sci.* **6** 15-50
- [39] Kresse G and Furthmüller J Efficient iterative schemes for ab initio total-energy calculations using a plane-wave basis set 1996 *Phys. Rev. B* **54** 11169
- [40] Blöchl P.E. *Phys. Rev. B* **50** 17953-17979 (1994).
- [41] Kresse G and Joubert D From ultrasoft pseudopotentials to the projector augmented-wave method 1999 *Phys. Rev. B* **59** 1758
- [42] Klimeš J, Bowler D R and Michaelides A Chemical accuracy for the van der Waals density functional 2010 *J. Phys.: Condens. Matter* **22** 022201
- [43] Klimeš J, Bowler D R and Michaelides A Van der Waals density functionals applied to solids 2011 *Phys. Rev. B* **83** 195131
- [44] Makov G and Payne M C Periodic boundary conditions in ab initio calculations 1995 *Phys. Rev. B* **51** 4014
- [45] Sato N, Inokuchi H and Silinsh E A Reevaluation of electronic polarization energies in organic molecular crystals 1987 *Chem. Phys.* **115** 269.
- [46] Endres R G, Fong C Y, Yang L H, Witte G and Wöll Ch Structural and electronic properties of pentacene molecule and molecular pentacene solid 2004 *Comput. Mat. Sci.* **29** 362-370.
- [47] G. Malloccia G, Cappellinia G, Mulasb and A. Mattonia Electronic and optical properties of families of polycyclic aromatic hydrocarbons: A systematic (time-dependent) density functional theory study 2011 *Chem. Phys.* **384** 19-27.

[48] The standard deviation for the out-of-plane distances of the atoms in the adsorbed pentacene molecule is less than 0.05 Å.